Journal of Controlled Release 196 (2014) 197–207

Contents lists available at ScienceDirect

Journal of Controlled Release

journal homepage: www.elsevier.com/locate/jconrel

Macromolecular (pro)drugs with concurrent direct activity against the hepatitis C virus and inflammation

Benjamin M. Wohl [a,b], Anton A.A. Smith [a], Bettina E.B. Jensen [a], Alexander N. Zelikin [a,b,*]

[a] Department of Chemistry, Aarhus University, Aarhus C 8000, Denmark
[b] iNANO Interdisciplinary Nanoscience Centre, Aarhus University, Aarhus C 8000, Denmark

ARTICLE INFO

Article history:
Received 14 August 2014
Accepted 15 September 2014
Available online 16 October 2014

Chemical compounds studied in this article:
Ribavirin (PubChem CID: 37542)
Poly(acrylic acid) (PubChem CID: 6581)
Poly(methacrylic acid) (PubChem CID: 3255932)
Poly(*N*-vinylpyrrolidone) (PubChem CID: 6917)
Poly(*N*-(2-hydroxypropyl) methacrylamide) (PubChem CID: 38622)

Keywords:
Macromolecular prodrugs
Polymer therapeutics
Ribavirin
Antiviral
Drug delivery
Hepatitis C

ABSTRACT

Macromolecular prodrugs (MPs) are a powerful tool to alleviate side-effects and improve the efficacy of the broad-spectrum antiviral agent ribavirin. In this work, we sought an understanding of what makes an optimal formulation within the macromolecular parameter space — nature of the polymer carrier, average molar mass, drug loading, or a good combination thereof. A panel of MPs based on biocompatible synthetic vinylic and (meth)acrylic polymers was tested in an anti-inflammatory assay with relevance to alleviating inflammation in the liver during hepatitis C infection. Pristine polymer carriers proved to have a pronounced anti-inflammatory activity, a notion which may prove significant in developing MPs for antiviral and anticancer treatments. With conjugated ribavirin, MPs revealed enhanced activity but also higher toxicity. Therapeutic windows and therapeutic indices were determined and discussed to reveal the most potent formulation and those with optimized safety. Polymers were also tested as inhibitors of replication of the hepatitis C viral RNA using a subgenomic viral replicon system. For the first time, negatively charged polymers are revealed to have an intracellular activity against hepatitis C virus replication. Concerted activity of the polymer and ribavirin afforded MPs which significantly increased the therapeutic index of ribavirin-based treatment. Taken together, the systematic investigation of the macromolecular space identified lead candidates with high efficacy and concurrent direct activity against the hepatitis C virus and inflammation.

1. Introduction

Ribavirin (RBV) is a broad-spectrum antiviral agent with proven activity against a number of RNA and DNA viruses, including influenza, hepatitis C (HCV) and Lassa fever viruses [1,2]. This drug appears on the World Health Organization list of essential medicines for both adults and children [3] and is the first line of defense against newly emerging viral infections. However, RBV has severe dose-limiting side effects such as accumulation of the drug inside red blood cells [4,5] and ensuing anemia, which precludes the wider use of this unique therapeutic. A historically successful approach to optimize the performance of drug molecules is with the tools of nanomedicine and in particular — protein and polymer conjugates [6–9]. For RBV, success has been documented using drug carriers such as hemoglobin, poly(L-lysine), and synthetic polymers [10–12]. For the former, the developed drug delivery strategy produced promising results *in vivo*, highlighting the potential of macromolecular prodrugs (MPs) as tools for the delivery of RBV [11].

In our work, we are interested in fully synthetic drug carriers, specifically due to the wide macromolecular parameter space and the associated synthetic and biomedical opportunities [13]. A major advantage of polymers is their versatility in regard to polymer molar mass (M_n), drug loading, and chemical characteristics of the carrier. Using these tools, it is possible to define the blood residence time of the conjugate and navigate the carrier to the nominated part of the body using targeting molecules [6,7,9]. By further relying on the arsenal of tools of bioconjugate chemistry [8], it is possible to define the drug release kinetics and achieve this through spontaneous hydrolytic mechanisms or in response to specific triggers, such as the activity of the chosen proteases. Polymer therapeutics can be obtained through the well-developed approach of polymer-analogous reactions, *i.e.* conjugation of the drug to the preformed reactive polymer chain, and this strategy is popular for the synthesis of anti-cancer MPs [9,14]. This strategy is not appealing for the synthesis of MPs of RBV since the latter offers only limited opportunities in direct conjugation (*i.e.* through the available 5′-hydroxyl). Alternatively, this nucleoside analog can be used to obtain its polymerizable derivatives such that MPs are then obtained through co-polymerization with a nominated co-monomer [13,15–17]. In our previous work, we synthesized the acrylate and methacrylate derivatives of RBV and successfully polymerized this monomer into a series of MPs [12,18,19]. Using fluorescently

* Corresponding author at: Langelandsgade 140, DK-8000, Aarhus C, Denmark. Tel.: +45 23297986.
E-mail address: zelikin@chem.au.dk (A.N. Zelikin).

http://dx.doi.org/10.1016/j.jconrel.2014.09.032
0168-3659/

labeled polymers we showed that conjugation to a carrier suppressed the association of RBV with erythrocytes to minimal levels. In contrast, MPs exhibited pronounced association with cells with hepatic relevance, namely hepatocytes and macrophages [17,18]. In doing so, MPs alleviate the origin of the main side effect of RBV.

Hepatocytes are the main cell type in the human liver and comprise the site of viral replication for HCV, and are therefore the prime therapeutic target. However, experiments with live infectious HCV can be performed only in highly specialized laboratories — in stark contrast to routine cell culture experiments which satisfy the needs of the basic *in vitro* characterization of *e.g.* anticancer MPs. Recently, an opportunity to optimize the drugs against HCV was brought to practice based on the non-infectious subgenomic replicon system of HCV [20]. This system makes it possible to study the impact of therapeutic agents on replication of the viral RNA in hepatocytes. The replicon is composed of an RNA construct (see Fig. 1) incorporating the non-structural components of the HCV virus, typically in combination with a reporter system and selection marker. The replicon employed in this study is based on a genotype 1b isolate (Con1, Ref. [21]), the most predominant HCV genotype worldwide. The replicon sequence also encodes a renilla luciferase for a facile readout of cellular viral levels. The entire RNA sequence is stably expressed within a human hepatocyte cell line (HuH7) and therefore allows for studying the influence of therapeutic agents on the intracellular viral life cycle (*i.e.* transcription and RNA replication). Importantly, this system does not produce infectious particles and as such the extracellular part of the viral life cycle (*i.e.* cell binding and uptake, release of viral particles) is of no influence, and the system can be employed under standard cell culture conditions. In our recent report, we revealed that this replicon system responds to the RBV treatment and is characterized with activity-related EC_{50} and toxicity-related IC_{50} values of 80 and 103 μM, respectively [22]. The established EC_{50} value is in large excess of the clinical concentrations of this drug (*i.e.* ~10–20 μM) [1,23] — thus contributing to the skepticism regarding the direct activity of RBV on HCV in clinic [2]. These values also illustrate a dramatically narrow therapeutic window for such a treatment. With the use of MPs of RBV, we were able to interfere with the replication of viral RNA with activity well exceeding that of RBV taken at clinical concentration — and with minor associated toxicity [22]. Success of this undertaking was due to the engineered linkage between the drug and the polymer (disulfide linkage coupled with a self-immolative linker). To our knowledge, this was the first report on direct inhibition of synthesis of the HCV genome using synthetic MPs of RBV.

From a different perspective, while RBV may not even exert a direct anti-HCV activity, [2] the activity of this drug as an inhibitor of inosine monophosphate dehydrogenase (IMPDH) leads to diverse downstream effects with relevance to the performance of RBV as a broad-spectrum antiviral agent [24,25]. Specifically, the depletion of the pool of intracellular guanosine triphosphate limits the synthesis of the viral nucleic acids, and this mechanism is relevant to the therapeutic effect of RBV against most viruses. For HCV in particular, it is hypothesized that a subsequent, further downstream event is more important, namely depletion of intracellular tetrahydrobiopterin (BH_4), a cofactor for inducible nitric oxide synthase (iNOS), thus resulting in inhibition of the synthesis of nitric oxide (NO) [26]. Over-expression of NO (activated by the presence of the virus) leads to persistent inflammation and hepatitis, and also decreases the activity of the cellular immune defense mechanisms [26,27]. Taken together, the activity of RBV as an inhibitor of NO synthesis appears to be highly relevant to the treatment of hepatitis. This therapeutic effect is also easy to quantify through routine cell culture experiments using macrophages as mimics to the liver-resident Kupffer cells [19]. Using this tool, we revealed that administration of MPs of RBV decreases the cellular production of NO and thus, MPs are effective in delivering their payload [12,19]. In summary, our prior research on MPs of RBV using the anti-inflammatory activity of this drug revealed that i) MPs decrease the toxicity of RBV and in doing so ii) may extend the therapeutic window of treatment; iii) polymer molar mass is

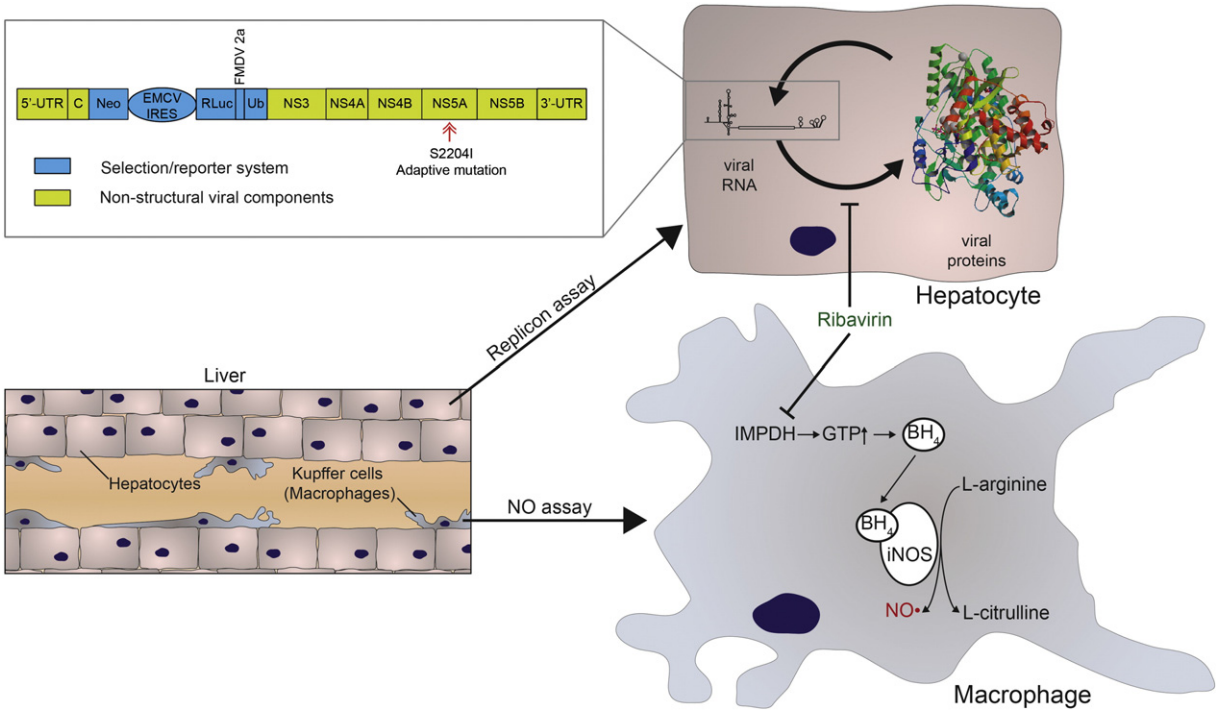

Fig. 1. Schematic illustration of the human liver and its major components, hepatocytes and Kupffer cells (macrophages). Based on these two cell types two model *in vitro* systems were employed in this study. Firstly, a subgenomic replicon composed of the non-structural components of an HCV genotype 1b isolate and a luciferase reporter system. Secondly, murine macrophages stimulated to produce nitric oxide through the addition of lipopolysaccharide. In the replicon assay ribavirin inhibits replication of the viral RNA, thus modeling the clinical treatment. The mechanism by which RBV elicits this effect is subject to debate. In stimulated macrophages ribavirin (more correctly its phosphorylated form) inhibits ionosine monophosphate dehydrogenase (IMPDH), leading through a cascade of events to the inhibition of nitric oxide production. In combination, the two assays allow for studying the intracellular activity of ribavirin on the two major hepatic cells *in vitro*.

important with regard to the therapeutic activity of the MPs; and iv) polyanionic carriers contribute to the therapeutic effect.

The aim to this work was to provide a systematical investigation of the macromolecular parameter space associated with MPs of RBV and to identify which polymer composition, *i.e.* structure of the polymer, molar mass, drug loading, makes the most favorable formulation. To accomplish this, we establish the therapeutic window and the therapeutic indexes of the MPs in the anti-inflammatory assay and choose lead formulations with optimized performance. Further novelty of this work lies in that we analyze the longevity of drug action and reveal that following a single dose administration, MPs significantly extend the duration of the observed therapeutic response. Finally, we put the MPs to a test in a HCV model based on the sub-genomic replicon of this virus and reveal, for the first time, that polyanionic carriers have an intracellular, direct activity against HCV. With RBV functionalization, efficacy of MPs in preventing replication of the viral RNA far exceeded that achieved by RBV (for safe, non-toxic treatment) and closely matches that achieved by high doses of interferon. Taken together, we were able to identify MPs with both, a direct activity against the virus *and* activity against hepatitis (liver inflammation). We anticipate that this data will prove useful for the development of safer antiviral treatments using the unique broad spectrum antiviral agent, ribavirin.

2. Materials and methods

If not stated otherwise all chemicals were purchased from Sigma-Aldrich and used as received. RAW 264.7 (ECACC, murine macrophage cell line) were routinely cultured at 37 °C and 5% CO_2 in full Dulbecco's Modified Eagle Medium (DMEM, 10% fetal bovine serum (FBS, Invitrogen, <5 EU/mL) and 1% penicillin/streptomycin, P/S) and passaged with a cell scraper. The Con1/SG-Neo(I)hRlucFMDV2aUb replicon system (Apath, USA) in HuH7 (human hepatoma cell line) was maintained in full DMEM media (DMEM, 10% FBS, 1% non-essential amino acids, 1% P/S, 500 μg/mL geneticin) and passaged according to the supplier protocol through trypsinization. If not stated otherwise, all absorbance, fluorescence and luminescence measurements were performed on a Perkin-Elmer Enspire plate reader.

2.1. Monomer synthesis

Ribavirin acrylate was synthesized as reported previously through a chemi-enzymatic route [12,17]. In short, ribavirin (APIchem, China) and enzyme beads (Nz435, Novozymes, Denmark) were suspended in dioxane with a few crystals of di-*tert*-butyl methylphenol. Following addition of acetoneoxime acrylate and reaction for 32 h at 50 °C the final product was obtained through column purification. Ribavirin methacrylate was synthesized analogously using acetoneoxime methacrylate.

2.2. Polymer synthesis and characterization

All polymers (except for those based on *N*-vinylpyrrolidone) were synthesized on a Chemspeed Swing-SLT platform *via* the reversible addition–fragmentation chain transfer (RAFT) polymerization relying on monomer/monomer ratios, monomer/RAFT ratios, and polymerization times as established previously. For full experimental details on the synthesis of the polyacids [12] and PVP [19] see our earlier publications. The synthesis of the HPMA library has in the meantime been accepted for publication [54]. In short, HPMA polymers were obtained using 4-cyano-4-[(dodecylsulfanylthiocarbonyl)sulfanyl]pentanoic acid as a RAFT agent, and polymerizations were performed in DMSO. Fluorescent analogs were prepared through the addition of 2 equivalents of fluorescein methacrylate in respect to the RAFT agent. Stock solutions of the ribavirin monomer, HPMA, RAFT agent, fluorescein and initiator were degassed through sparging with nitrogen for 15 min. The stock solutions were robotically aliquoted into the reaction vessels. Resulting mixtures were degassed by four freeze-evacuate–thaw cycles. The mixtures were heated with agitation for the specific time (12–24 h, depending on monomer/RAFT ratio, for HPMA) [12,19]. The polymers were recovered by precipitation into a 2:1 mixture of ether and acetone, followed by filtering and vigorous washing with acetone. Characterization of the polymers was performed using size-exclusion chromatography (SEC) consisting of a LC-20AD Shimadzu HPLC pump, a Shimadzu RID-10A refractive index detector and a DAWN HELEOS 8 light scattering detector along with a Shimadzu SPD-M20A PDA detector, equipped with a HEMA-Bio Linear column with 10 μm particles, a length of 300 mm and an internal diameter of 8 mm from MZ-Analysentechnik in series with a OHpak SB-803 HQ Shodex column with the dimensions 8.0 × 300 mm and a particle size of 6 μm. The eluent was water filtered through a 0.1 μm filter and supplemented with 300 ppm sodium azide.

2.3. RAFT end-group removal

The RAFT Z-group was removed from the HPMA polymers by dissolving 20 mg of the polymer in 0.2 mL of a non-buffered 1 g/L solution of $NaBH_4$, followed by precipitation into acetone. For acrylic and methacrylic acid polymers, end-group removal was accomplished through radical cross-coupling [28]. In a typical experiment, a polymer sample was dissolved in DMF. The solution was charged with 20 mole equivalents of AIBN with respect to the RAFT agent, followed by sparging of the solution for 20 min with nitrogen and heating the mixture to 65 °C for 10 h. The polymers were recovered by precipitation into DCM. Removal efficiency for the RAFT Z-group was quantified by dissolving the respective polymer and their untreated precursor at 10 g/L in water and measuring absorbance at 310 nm (Thermo Fisher Scientific Nanodrop 2000c). The percent removed RAFT group was calculated from the blank corrected absorbance values of the two corresponding polymers.

2.4. Therapeutic effects in macrophages

The intracellular activity of ribavirin in macrophages was measured through its inhibitory activity on NO production in stimulated macrophages [19]. In a clear 96-well plate 20,000 RAW 264.7 cells/well were seeded (100 μL of media). Following cellular attachment (3–4 h) the specific agents (*i.e.* RBV, MPs, AZT) were added in triplicate on each plate at the specified concentration and incubated for 24 h. Where necessary, polymer solutions (acrylic and methacrylic acid polymers) were neutralized previous to the addition to cells. Cells were stimulated through the addition of 1 μg/mL of lipopolysaccharide (LPS, *Escherichia coli* 026:B6) to refreshed media. Relative NO levels were determined following further 24 h of incubation from the cell supernatant through the Griess assay [29] and a freshly prepared sodium nitrite standard curve. The viability of the retained cells was quantified through the PrestoBlue assay (Invitrogen) according to the manufacturer's protocol by determining fluorescence levels following 30 min of incubation at 37 °C in refreshed media. Viability and NO levels were normalized to a negative control of LPS treated cells. Ribavirin (10 μM) and L-N^G-nitroarginine methyl ester (1 mM) were included as positive controls in every experiment.

2.5. Confocal laser scanning microscopy

For visualization of polymer uptake 100,000 cells/well (1 mL, RAW 264.7) were seeded into a 12-well plate with round glass slides (⌀ 16 mm). After 24 h media were refreshed and polymers added to a final concentration of 1 g/L. Where necessary, polymer solutions were neutralized previous to the addition to cells. Following further 24 h of incubation the cells were washed with phosphate buffered saline (PBS, 500 μL) and fixed with paraformaldehyde (4%, 500 μL, 10 min). The excess fixing agent was removed through two PBS washes and subsequently the cell nuclei were stained with 4′,6-diamidino-2-phenylindole (10 μg/mL, 450 μL, 5 min), followed by

two PBS washes. Glass slides with cells were mounted (Vectashield mounting medium) onto cover slides and sealed and fluorescent imaging was performed on a Zeiss confocal laser scanning microscope, LSM 710.

2.6. Durability of therapeutic activity in macrophages

RAW 264.7 cells were seeded, treated and stimulated analogously to the standard protocol (see above) at a final polymer concentration of 0.1 g/L. 24, 48, and 72 h following LPS stimulation NO levels were assayed in the aspirated cell media of each well through the Griess assay. Cell media above the cells were refreshed and cell culture was continued. At the 72 hour time point, the viability of the cells was quantified using the PrestoBlue viability assay.

2.7. Antiviral therapeutic effects in hepatocytes

Effects of (pro)drugs against viral RNA replication were quantified using a HCV subgenomic replicon system. 6000 cells/well (100 μL) of HuH7 cells harboring the replicon were seeded into a white 96-well plate. After 2–3 h, following cellular attachment, the media were refreshed to remove the selection agent geneticin (G418) from the cells. Cells were incubated in the absence of G418 from here on. The agent of interest was added in triplicate on each plate to achieve the desired final concentration and the cells were incubated for further 48 h. Where necessary, polymer solutions were neutralized previous to the addition to cells. Subsequently, cell media were refreshed (50 μL) and a PrestoBlue viability assay was conducted (10 μL, 60 min, 37 °C). Fluorescence levels are determined in a separate well plate and remaining cells washed with PBS. To 50 μL of fresh media, 50 μL of luciferase assay reagent was added (Promega, Renilla-Glo) and luminescence was read out after 10 min of incubation. Viability and luminescence were normalized to an untreated cell sample.

2.8. Data processing

All results were analyzed in Microsoft Excel and plotted in OriginPro. Statistical significance between samples was determined through a heteroscedastic two-tailed T-Test (Excel). Sigmoidal fitting functions were applied to dose–response curves with OriginPro using the formula $y = A_1 + \frac{A_2 - A_1}{1 + 10^{(LOGx0 - x)p}}$, with LOGx0 and p as fitting parameters and A_1 and A_2 the bottom and top asymptotes, respectively. LOGx0 marks the midpoint between the asymptotes and as such EC_{50} and IC_{50} values are defined by the coordinates $(LOGx0, (A_1 + A_2)/2)$. The sigmoidal function was fit to the experimental data points using an iterative Levenberg–Marquardt algorithm until the fit converged and the tolerance criteria (as defined by OriginPro) were satisfied.

3. Results and discussion

The power of macromolecular prodrugs lies in their ability to mask the attached drug from the bodies' "senses" and drastically change the distribution of the drug. The pharmacokinetic profile of the polymer is conferred to the drug, and this phenomenon is beneficial in the development of *e.g.* anti-cancer therapeutics. From a different perspective, polymer carriers with matched molar mass and drug loading may exhibit vastly different cellular internalization behavior and/or drug release kinetics, all of which will ultimately result in an altered activity of the drug. With the overall goal to identify the most favorable polymer composition for optimized intracellular delivery of RBV, we used a broad selection of polymers based on four monomers, namely *N*-vinylpyrrolidone, *N*-(2-hydroxypropyl) methacrylamide, acrylic acid, and methacrylic acid (Fig. 2) [12,19,54]. The corresponding polymers (PVP, PHPMA, PAA, and PMAA) have documented characterization in biomedicine with utility in drug delivery and, for polyanionic carriers, antiviral research [13]. As a starting point for the side-by-side

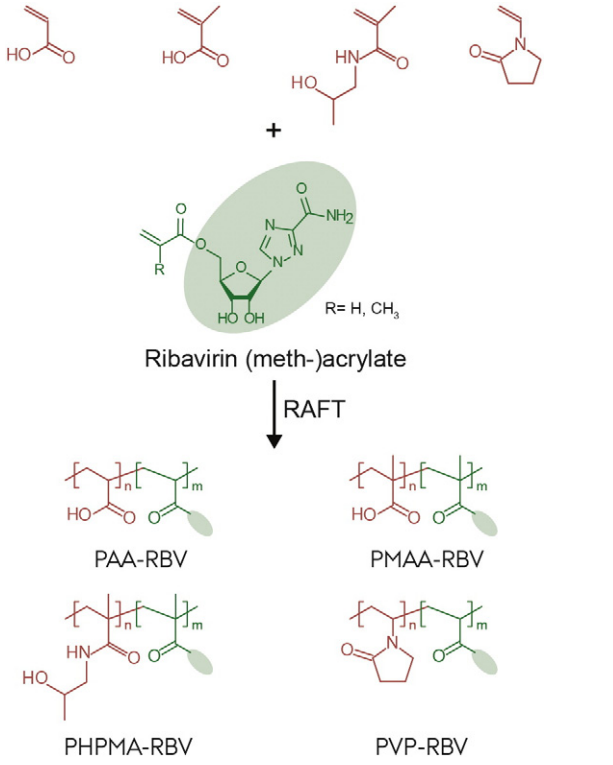

Fig. 2. Synthesis of macromolecular prodrugs of ribavirin using different comonomers and RAFT controlled polymerization to obtain polymers with controlled molar mass and drug loading. See Fig. SI1 for details.

characterization of the carriers, we used polymers with closely matched molar masses and drug loading (~8 kDa and 10 mol% RBV, respectively, Table SI1) [12,19]. Polymers were obtained using a controlled polymerization technique, RAFT, and had low dispersity thus allowing for sound structure–function correlations.

Macromolecular prodrugs were first used in an anti-inflammatory model, *i.e.* as inhibitors of the synthesis of nitric oxide by stimulated macrophages. Therapeutic effect and associated toxicity were evaluated in a concentration range from 31 mg/L to 1 g/L (Fig. 3, top row). Select data points for PVP from our earlier publication [19] were included in Fig. 3 for direct comparison. An immediate observation is that the four polymers elicited drastically different therapeutic responses. Each carrier sustained a drug activity at a high administered dose (1 g/L polymer concentration), and each polymer revealed a well-pronounced dose–response. However, at the lowest concentration tested, only the PAA-based MP had a significant therapeutic activity (~50% inhibition of NO synthesis). This observation provides the first indication that success in delivery of RBV by its polymer-based carrier is largely dependent on the nature of the carrier. In this row of MPs, PAA proved to be the most potent formulation. Interestingly, PMAA is a structurally similar polyanion but showed a markedly lower activity. PAA and PMAA are weak polyanions and their degree of ionization is a function of pH. The pKa of PMAA is one to two units of pH higher than PAA (6.5 *vs.* 4.5 respectively), leading to a significantly lower anionic charge for PMAA at physiological pH. This might explain the observed similarity between the activity profile of PMAA and PHPMA and the difference to the highly polyanionic PAA. Further important observation is that, as with RBV, the therapeutic activity of MPs is followed by the cytotoxic effect. However, for each MP tested, there is a concentration range in which there is a pronounced, statistically significant inhibition of synthesis of NO without an accompanying toxicity. As visualized using reference lines in Fig. 3, this cannot be achieved with the free drug (see Ref. [19] for further details) and illustrates the benefit of RBV delivery using polymers.

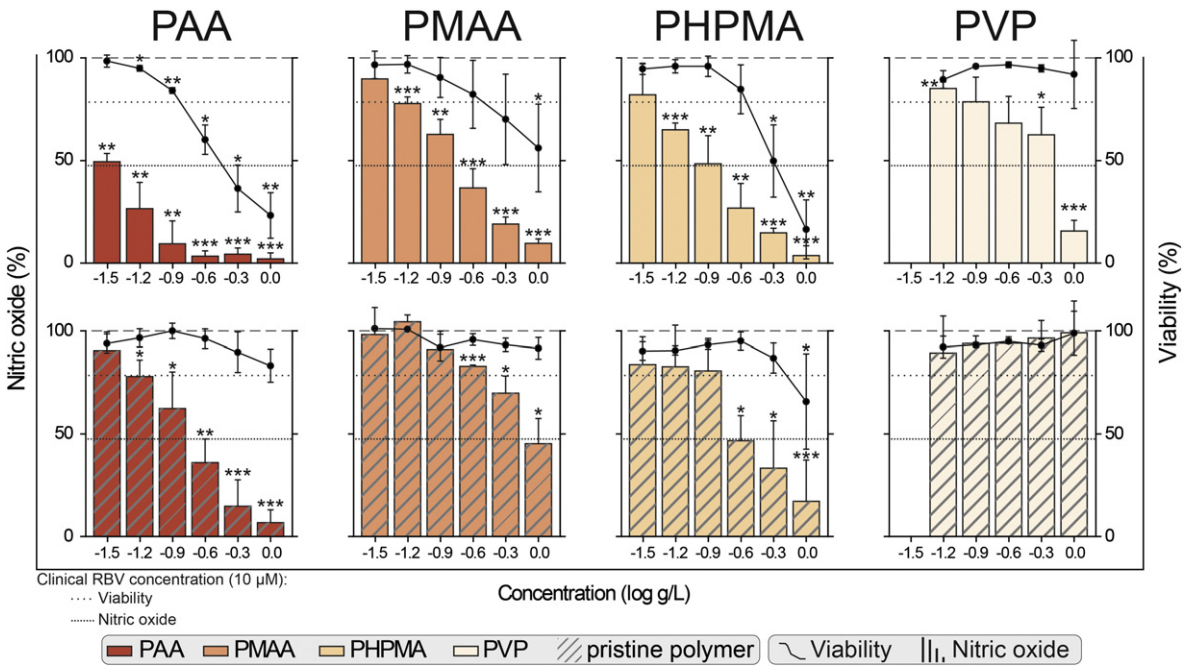

Fig. 3. Dose-dependent inhibition of NO production by polymer prodrugs based on various carriers both for macromolecular prodrugs (top row) and pristine polymers (bottom row). Data for PVP was adapted with permission from (Wohl et al. [19]) for illustrative purposes. Copyright (2013) American Chemical Society. Shown results are the mean ± SD of at least three independent experiments ($n \geq 3$). Statistical significance is given compared to the negative control. *$P < 0.05$, **$P < 0.01$, and ***$P < 0.001$.

The production of nitric oxide is a highly regulated pathway and as such has numerous therapeutic targets to suppress the production of NO [30]. Following cellular inflammation (virus- or bacteria-induced or using lipopolysaccharide, LPS), possible routes of intervention can be grouped into inhibition of transcription factors (*e.g.* NFκB, STAT-1α, IRF-1), iNOS and iNOS mRNA destabilization, as well as the regulation of required substrates (*e.g.* L-arginine) and cofactors (*e.g.* BH_4). Inhibition of NO synthesis by RBV has its mechanism in the latter opportunity, *i.e.* depletion of the iNOS cofactor, BH_4 [31]. We have previously observed that polyanionic carriers also exhibit activity in suppressing the synthesis of NO [12]. Furthermore, dithiocarbamate compounds are known blockers of the iNOS activation pathway (*via* blocking of NF-κB) [32]. These compounds are structurally similar to the terminal groups as found on polymers obtained *via* the RAFT mechanism such as those used for all the polymers in this work (Fig. SI1). Even though these groups make up a rather small part of the overall polymer structure, it has been demonstrated that the RAFT group can elicit cellular toxicity [33,34]. Taken together, this identifies three different components that might play a role in the overall effect observed: the polymeric carrier, the conjugated drug, and polymer end-groups.

3.1. Polymers as inhibitors of nitric oxide synthase

Anionic polymers (polyanions) are abundant in nature (nucleic acids, heparin, hyaluronic acid, etc.) and have a diversity of functions. Their synthetic analogs, including PAA and PMAA, have also exhibited a magnitude of physiological effects, including inhibition of the viral cell entry, [13] stimulation of the production of interferon [35,36], and adjuvant activity [37]. In our recent communication, we observed that short chains of PAA are effective inhibitors of the synthesis of NO [12]. Herein, the four pristine polymers, *i.e.* polymers corresponding to the MPs discussed above but without conjugated drug, were used to obtain the dose–response curve in the same concentration range (Fig. 3, bottom row). PAA, PMAA, and PHPMA but not PVP proved to be efficient inhibitors of the production of nitric oxide by stimulated macrophages. Interestingly, the therapeutic effect was almost devoid of corresponding cytotoxicity (except for the highest polymer concentration tested, 1 g/L). Perhaps the most unexpected result is that PHPMA exhibits a pronounced, statistically significant intracellular effect and afforded ~50% decreased levels of NO at concentrations as low as 0.25 g/L. At present, we cannot offer any mechanistic explanation to this phenomenon. Nevertheless, for each of the polymers investigated in Fig. 3, it holds true that with matched concentration, therapeutic activity for MPs is higher than that observed for the corresponding pristine polymer — and this illustrates that delivered RBV has an intracellular activity. At the same time, the polymers themselves have an inherent activity in the assay and the carrier macromolecule appears to contribute to the overall therapeutic effect. Notably, the activity of the pristine polymers had minor if any associated toxic effects — in contrast to the activity of RBV in this assay, which is characterized by a very narrow therapeutic window (*vide infra*).

3.2. RAFT end-groups do not contribute to the inhibition of iNOS

To investigate the influence of polymer end-groups inherited with the mechanism of synthesis, RAFT Z-groups were removed from pristine PAA and PMAA polymers through radical cross-coupling with the initiator, AIBN [28,38] (Fig. 4A). The RAFT agent of PHPMA was removed through treatment with $NaBH_4$. Removal efficiency was over 80% for all polymers as quantified through UV absorbance at 310 nm, a signature of the RAFT group (Fig. 4B). For all three carriers, the samples with and without the RAFT end-group were tested for their inhibitory activity in the NO synthesis assay (Fig. 5A). Additionally, a commercially available sample of PMAA (18.7 kDa) was included in this analysis. For PAA and PMAA, no significant differences were observed for polymers with and without the RAFT group. For PHPMA, removal of the RAFT group decreased the activity of the polymer but with no statistical significance.

As a further, final test to probe the active ingredient (the drug, the polymer, or the terminal groups), we also tested side by side two samples of PHPMA equipped with two antiviral drugs, RBV and azidothymidine (AZT) [39]. The latter therapeutic is active against the human immunodeficiency virus but has no effect on the synthesis of NO by stimulated macrophages (except at millimolar concentrations by inhibiting the overall cellular metabolism, Fig. SI3). At matched molar mass and drug loading and the same terminal groups, the PHPMA–AZT sample had no activity in suppressing the synthesis of NO whereas

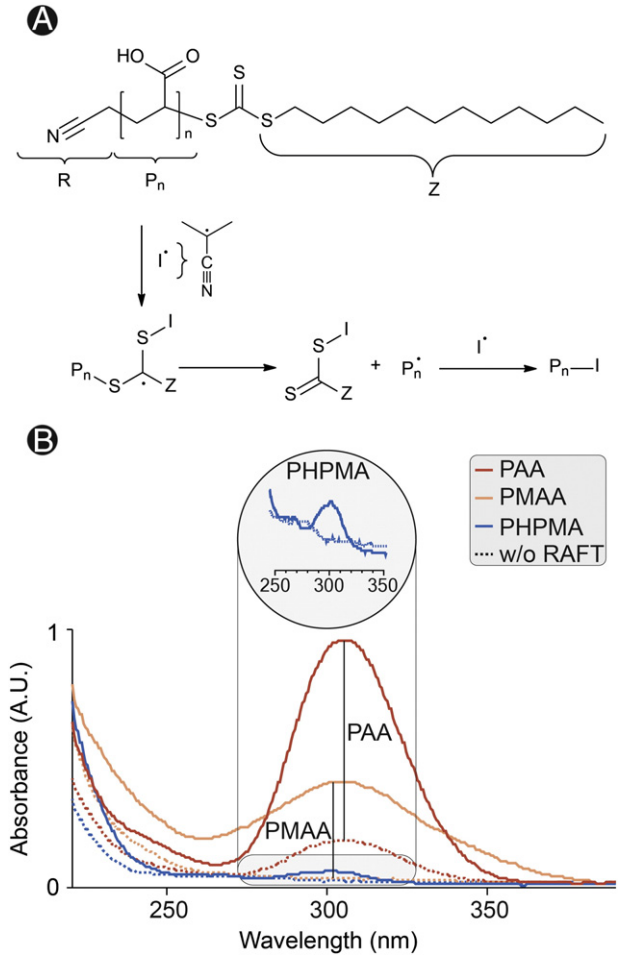

Fig. 4. A) Scheme of RAFT group removal from polymers through radical cross-coupling with initiator AIBN, illustrated on PAA. For structure of other carriers see Fig. SI1. B) Absorbance spectra of PAA, PMAA, and PHPMA polymers before and after RAFT group removal. See Table SI2 for polymer characteristics and removal efficiency.

PHPMA–RBV revealed a significant activity (Fig. 5B). Thus, for PHPMA, it stands that the therapeutic effect is due to the conjugated RBV, to some extent due to the PHPMA backbone, and is not an inherent feature associated with the method of polymer synthesis. For PAA, PMAA, and PHPMA alike, our current data do not allow for a conclusion as to how pristine polymers regulate the synthesis of NO. A detailed investigation of the involved cellular pathways warrants further study and is the subject of our ongoing research.

3.3. Structure–function correlation within the macromolecular parameter space

To investigate the interplay between therapeutic activity and cellular toxicity, dose–response curves as presented in Fig. 3 were obtained for a total of 21 polymers with systematically varied composition (Fig. 6). Polymer set A contained polymers with closely matched molar mass and drug loading and differed in the chemistry of the backbone. Set B was assembled using polymers with matched backbone (PAA or PHPMA) and drug loading and differed in average molar mass of the MPs. Set C was organized such that molar mass was kept constant and only RBV content was varied, from 0 to ~20 mol%. For each polymer, dose–response curves were used for mathematical fitting to determine the activity (EC_{50}) and associated toxicity (IC_{50}) effects (see Fig. SI4 for full dose–response curves and fitting functions). Comparative analysis of the (pro)drugs was then performed using three metrics, namely the therapeutic window (TW) in terms of polymer concentrations, the

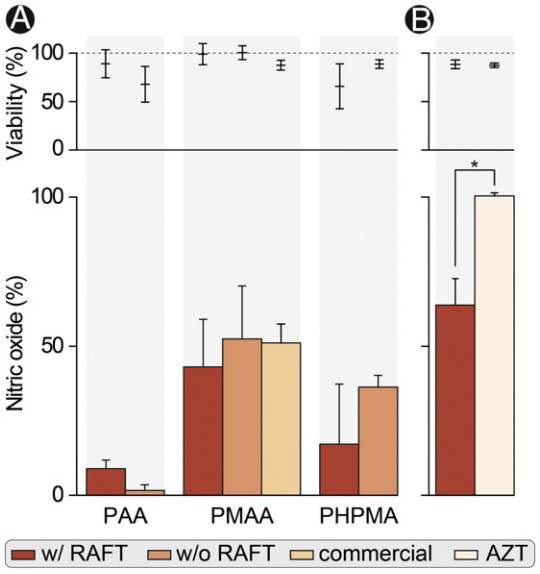

Fig. 5. A) Comparison of therapeutic activity and cellular viability of PAA, PMAA, and PHPMA polymers before and after RAFT group removal at 1 g/L. Commercial PMAA (18.7 kDa) was obtained from Sigma-Aldrich. See Fig. SI2 for comparison at 0.1 g/L and Table SI2 for polymer characteristics. Shown results are the mean ± SD of four independent experiments (n = 4). B) Comparison between a PHPMA–RBV and a PHPMA–AZT conjugate of matched molar mass and drug loading at 0.1 g/L. For polymer details see Table SI3. Shown results are the average of three independent experiments (n = 3). Statistical significance is given between the indicated samples. *P < 0.05.

therapeutic window in equivalent molar drug concentrations, and the therapeutic index (TI). These are graphically presented in Fig. 7 and discussed in detail below.

Visualization of the therapeutic window expressed in the overall w/v concentration allows for comparing the effects observed for individual formulations. This metric takes into account the contribution of the polymer (as well as inactive drug) in the overall effect. This consideration is important in that the amount of foreign material administered to the patient is meant to be kept as low as possible. In this regard PAA-based MPs achieve the highest potency with an EC_{50} value as low as 0.03 g/L. Furthermore, these data reveal that all things considered, the nature of the carrier polymer is the dominant factor defining the potency of the MPs. With matched molar mass and drug loading, PAA based formulations are the most potent as compared to their counterparts based on other polymer chemistries (Fig. 7I, set A). Compared to the effect of the carrier, the average molar mass of MPs exhibited a minor effect on the EC_{50} (see Fig. 7, set B). Indeed, shorter chains of

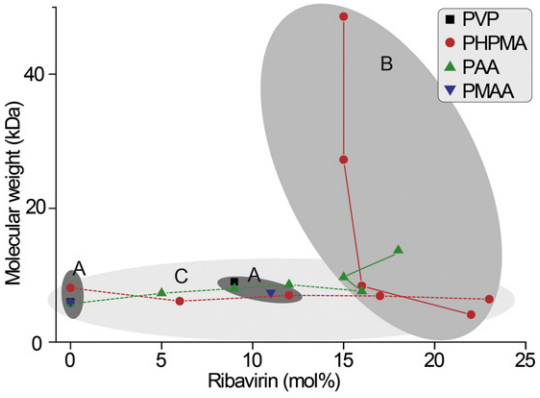

Fig. 6. Visual representation of molecular weight, drug loading, and carrier of polymer samples. The effect of polymeric carrier (set A), polymer molar mass (set B) and drug loading (set C) of the polymer samples was systematically studied. For characteristics of all studied polymers also see Table SI1.

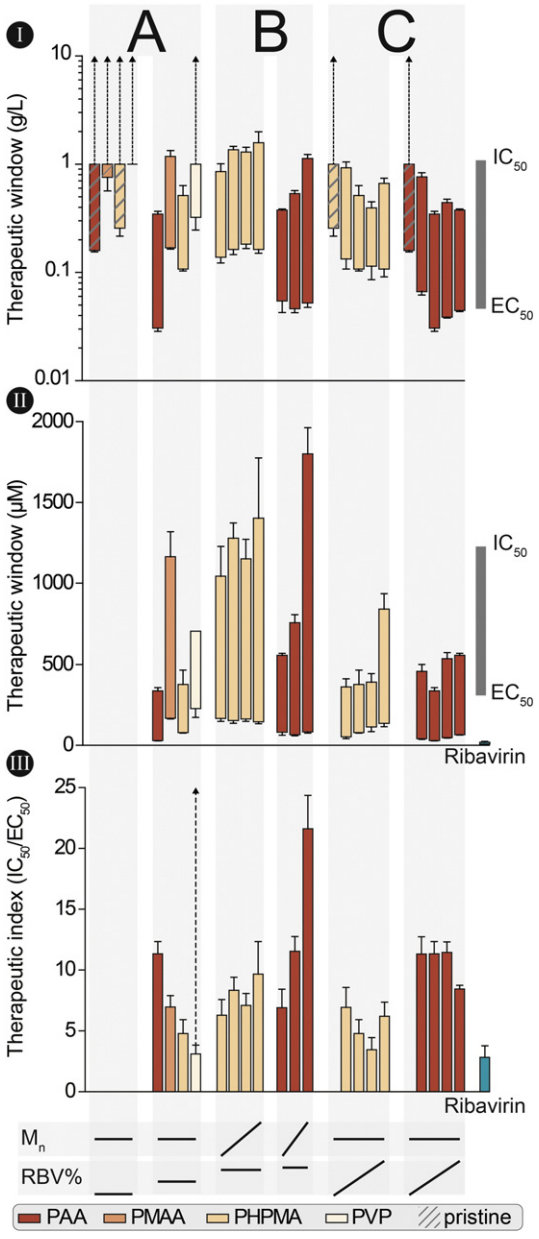

Fig. 7. Visualization of therapeutic window (difference between IC_{50} and EC_{50}) in polymer concentration (g/L) as well as equivalent molar drug concentrations for all studied polymers. Change in M_n and RBV content is shown for illustrative purposes for each series, for exact details of polymer characteristics see Table SI1. Therapeutic index (shown in bottom graph) was calculated through ratio of IC_{50}/EC_{50} in equivalent molar RBV concentrations, allowing for direct comparison to free RBV. IC_{50} and EC_{50} values ± SE were obtained from dose–response fitting functions as shown in Fig. SI4. For numerical values of IC_{50}, EC_{50}, and TI see Table SI4.

PHPMA were more potent – agreeing well with our previous finding on this subject [13] – yet no composition from this series is nearly as potent as the PAA counterpart with similar drug loading, regardless of M_n. Interestingly, the average molar mass appears to be more important when it comes to toxicity, and with increased chain length, polymers become less toxic (see set B). As a result, higher molar mass polymers reveal markedly broader TW in terms of w/v concentrations. With regard to drug loading (set C), variation in the content of RBV results in concurrent change in both, potency and toxicity of the formulation, and TW intervals appear to be quite similar for polymers with the same backbone and molar mass.

To obtain the therapeutic window in equivalent drug concentrations, the w/v concentrations of polymers were converted to equivalent molar concentrations of RBV based on the total drug content of the respective MP. Ribavirin requires intracellular phosphorylation at its 5′-hydroxyl to gain activity, the same hydroxyl used in conjugation to the polymer. Thus, for activity RBV has to be released from the carrier. The calculated TW in terms of equivalent concentration of RBV does not take into account the fact that MPs will only release a part of their therapeutic payload in the run of an experiment and therefore this metric is somewhat flawed. That said, this representation provides a visual comparison between the pharmacodynamic properties of MPs alongside pristine RBV (Fig. 7II). MPs result in a tremendous expansion of the therapeutic window in comparison to RBV itself. While for RBV the TW covers a concentration range of just 12 μM, TW for MPs covers a range of 300 to 1000 μM, giving a much larger flexibility during dosing. On the down side, this graph also demonstrates an apparent loss of activity associated with prodrugs due to partial drug release. This phenomenon is not unexpected and is quite typical for all formulations based on MPs [11,40–43]. In our case, most MPs required 10–20 times higher overall drug concentrations to achieve the same efficacy as the free drug. Nonetheless, the most potent MPs achieve an EC_{50} coming close to the free drug itself, illustrating the potential of identifying lead candidates through this study.

The therapeutic index is arguably a more stringent metric and is based on the ratio of IC_{50} to EC_{50}. For this criterion of comparison, PAA based MPs were also superior and afforded a 4 to 8-fold increase in the TI compared to pristine RBV (Fig. 7III). In contrast to the potency, the therapeutic index is clearly controlled by the polymer M_n for PAA, with higher indices obtained with increasing molecular weight. It has to be noted however, that PAA samples within this study are of a relatively narrow range of molecular weights (8 to 14 kDa). In contrast, PHPMA seems to be under stronger control by drug loading, with increasing drug loadings resulting in lowered TIs. According to this finding, higher drug loadings do not necessarily lead to a more favorable formulation. Even if the drug loading is associated with an increased potency, this is also associated with increased toxicity. Importantly, among the 15 MPs studied, 13 polymer compositions were characterized with at least a 2-fold higher value of TI compared to RBV and PAA sample with an M_n of 14 kDa and RBV content of 18 mol% exhibited a TI 8-fold that of RBV. Table 1 summarizes the main conclusions drawn from Fig. 7.

For select samples, we also performed visualization of cellular internalization of MPs using confocal laser scanning microscopy (CLSM) (Fig. 8). In these experiments, we used custom made, fluorescently labeled polymers (for details, see Table SI5). It has to be noted that fluorescence levels in cells upon polymer internalization should not be compared directly, as different MPs were characterized with different fluorescence intensities (*i.e.* fluorescence per unit mass, data not shown). For all polymers, it was possible to detect intracellular fluorescence indicating polymer uptake. Interestingly, the intracellular distribution of the fluorescence signal was different from one polymer to another. Thus, for PHPMA, PMAA, and PVP fluorescence is concentrated within tight clusters many of which are localized in the perinuclear area of the cell, indicative of the lysosomal trafficking and entrapment of MPs. In contrast, for PAA, the fluorescent signal is distributed much more evenly throughout the cell. Fluorescein was incorporated into

Table 1
Summary of main conclusions from Fig. 7 in regard to the influence of polymer molar mass and drug loading on formulation potency, formulation toxicity, width of the therapeutic window, and therapeutic index. An upward arrow indicates a positive correlation (*e.g.* increasing therapeutic index with increasing M_n). For each metric, a lead candidate that performed best was identified.

Metric	M_n	RBV loading	Lead candidate
Potency	→	↑	PAA, 8 kDa, 9 mol%
Viability	↑	↓	PAA, 8 kDa, 9 mol%
Therapeutic window	↑	→	PAA, 22 kDa, 20 mol%
Therapeutic index	↑	↓→	PAA, 22 kDa, 20 mol%

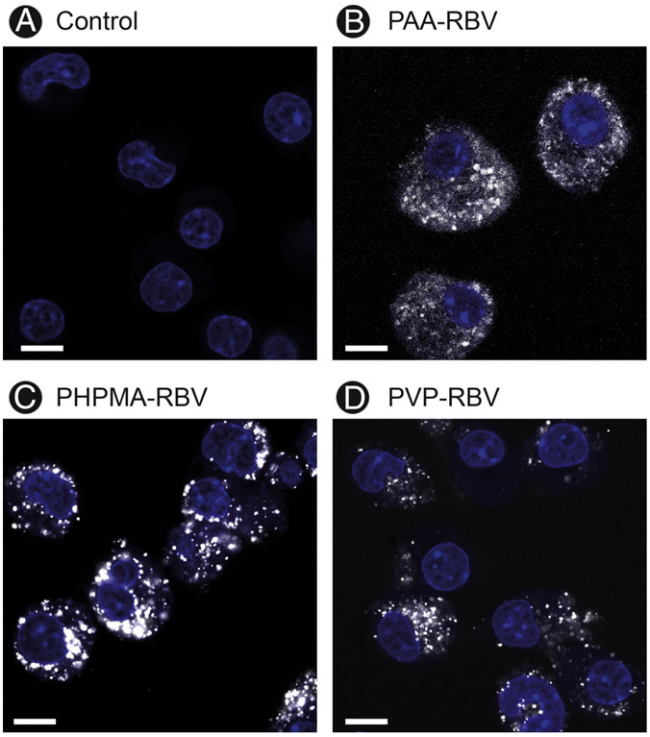

Fig. 8. Polymer uptake into macrophages as visualized through CLSM microscopy using fluorescently labeled polymers (see Table SI5). Cells were visualized following 24 hour incubation at 1 g/L of polymer. Scale bars correspond to 10 μm. Fluorescent intensity between samples should not be directly compared as MPs were characterized to have different fluorescent intensities. Images were optimized for each sample for better visibility of internalized polymers. For images with remaining polymers see Fig. SI5.

MPs using its acrylate derivative, *i.e.* having the same ester bond to the polymer as RBV. Distribution of fluorescein may indicate localization of MPs and/or the released dye (and hence, the drug). RBV exerts its activity in the cytosol, not the lysosome/endosome. Of the MPs studied, derivatives of PAA are most potent and also the only MP with a uniform intracellular distribution. This observation may be pointing towards the origin of the superior activity of PAA–RBV conjugates, namely efficient escape from the lysosomal pathway. However, to our knowledge, PAA does not possess inherent endosomolytic properties. This property requires the use of analogs with a greater hydrophobic character (such as polymers made of propyl acrylic acid) [44]. Another explanation may take into account the possibility of intramolecular acid catalysis to facilitate the hydrolysis of the ester bond between RBV (or fluorescein) and the polymer backbone. PAA is more acidic than PMAA and would be a more efficient catalyst. This may lead to an accelerated drug release compared to PMAA-, PHPMA-, and PVP-based prodrugs and higher activity (potency) of these conjugates, as is indeed observed in our experiments. This early indication of the intramolecular catalysis for drug release from MPs is intriguing and we are now investigating this as a tool to control drug delivery in detail.

3.4. Longevity of the therapeutic activity

One of the benefits made possible by the field of controlled drug delivery is an extended duration of therapeutic activity achieved through a gradual – not bolus – release of drug from a carrier [45]. For MPs, this is possible due to the continuous intracellular cleavage of the ester functionalities between RBV and the carrier. We have recently shown that MPs of AZT (an anti-HIV drug) inhibit viral infectivity over at least 48 h whereas the pristine drug lost all of its activity during this time [39]. To investigate this effect for MPs of RBV, (pro)drug activity was quantified 24, 48 and 72 h after LPS stimulation (Fig. 9A–C). Media were refreshed at each time point (including LPS stimulation) to remove non-internalized agents. For all the samples, cell viability was assayed at the final time point (72 h) and MPs were found not to elicit any toxic effects (Fig. 9D). Progression of therapeutic activity revealed that the pristine drug gradually loses its activity over 48 h and no activity was observed at 72 hour post-stimulation. Counter to expectation, MPs lost their activity in this timeframe at a similar rate regardless of the composition of the MP (polymer carrier, molar mass, drug loading). Thus, MPs do not appear to extend the duration of action of RBV. However, MPs appear to deliver the therapeutic benefit through a different mechanism. In contrast to the pristine drug, MPs allow a high level of initial activity of the formulation in the absence of noticeable cytotoxicity and even after 4 days in cell culture (72 h after LPS stimulation), these MPs reveal a pronounced, statistically significant decrease in the synthesis of NO (Fig. 9C). A similar approach (higher initial response) is not possible for RBV itself, as this requires an increased drug-dose associated with unacceptable toxicity.

3.5. Inhibition of viral RNA replication in hepatocytes

In the next set of experiments, we aimed to investigate the structure–function parameter space for MPs of RBV with regard to their capacity to interfere with the replication of the HCV replicon in hepatocytes. The classical treatment for hepatitis C consists of a combination of ribavirin and interferon-α (IFN-α) [2]. Even though new direct-acting antivirals have reached the market, RBV and/or IFN-α remain an integral part of the drug regimen required to achieve an effective treatment [46]. For the initial characterization of the replicon system, the activity of both RBV and IFN-α was investigated on the replicon system both for 24 and 48 h of incubation (Fig. SI7). Interferon effectively inhibited viral RNA replication

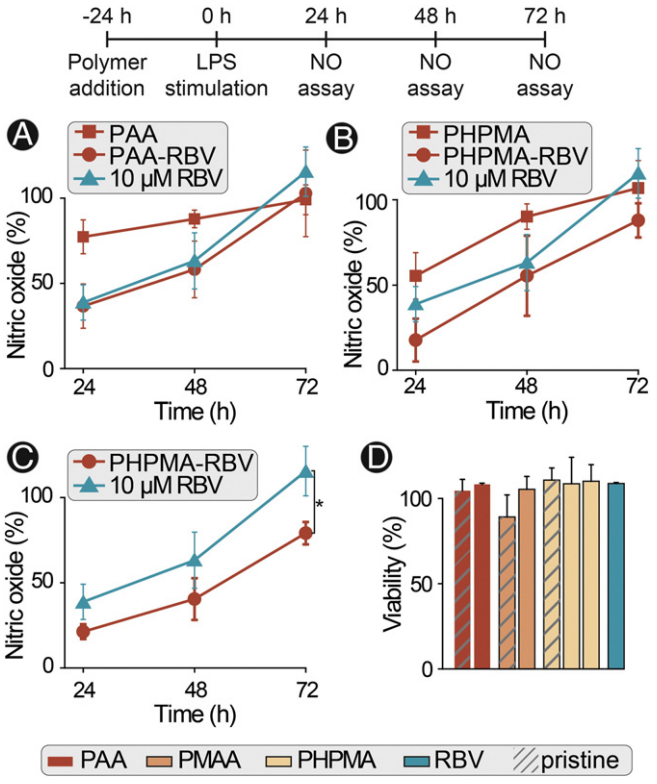

Fig. 9. Durability of therapeutic response of macromolecular prodrugs (0.1 g/L) in comparison to 10 μM of free RBV over 72 h. MPs and drug were added to cells 24 h prior to LPS stimulation. NO levels were measured in the cell supernatant every 24 h for the next 72 h. A) and B) Comparison of pristine polymer and polymer–drug conjugate for PAA (8 kDa, 9 mol%) and PHPMA (7 kDa, 12 mol%) with RBV. C) Macromolecular prodrug (7 kDa, 17 mol%) with strongest initial response in comparison to RBV. D) Viability for all polymers shown here after 72 h. Results are the average ± SD of five (A–C) or three (D) independent experiments ($n = 5$ or $n = 3$). Statistical significance is given between indicated samples. *$P < 0.05$. For data from all polymers see Fig. SI6.

without any toxic effects. Increased incubation times produced a markedly enhanced cellular response. With IFN-α, a 50% reduction in viral load was achieved at the cytokine concentration as low as ~1 U/mL, whereas clinical concentrations have been reported to be 40 to 116 U/mL [47]. In turn, RBV also elicited pronounced effects but at concentration of ~100 μM — in large excess of its clinical concentrations (*i.e.* 9 to 18 μM) [1,23]. Increasing the incubation time led to enhanced efficacy of treatment but not potency — a decrease in the viral levels was still not observed below 100 μM. At this time point, this high dose of RBV was associated with a pronounced toxicity of treatment. We have previously shown that further incubation of hepatocytes with RBV significantly aggravates toxicity in terms of magnitude of the toxic effect (at the same time, IC_{50} values changed rather little from 24 to 48 and further to 72 h of cell culture) [19]. Also, co-administration of IFN-α and RBV resulted in an additive effect of treatment. However, combination with INF-α too failed to increase the potency of RBV (data not shown). Through a more detailed dose–response curve for RBV at 48 h, we established the activity-related EC_{50} and toxicity-related IC_{50} values of 80 and 103 μM, respectively [22]. These values illustrate that RBV has a very narrow therapeutic window in this treatment — in fact, even narrower than in macrophages with regard to the inhibition of synthesis of NO [19].

3.6. MPs effectively inhibit viral RNA replication

To investigate the activity of MPs in the viral replicon system, polymers were allowed 48 h to elicit their therapeutic effect in the concentration range from 16 mg/L to 1 g/L, following which luciferase levels were quantified along with the cytotoxicity (Fig. 10A). In these experiments, we used MPs based on PAA (8 kDa, 9 RBV mol%) and PHPMA (7 kDa, 12 RBV mol%) along with the respective control polymers bearing no RBV. For PHPMA, the apparent antiviral effect was closely related to the overall toxicity of treatment and polymer activity in this assay was largely due to the decrease in the cell viability. Furthermore, surprisingly, polymer chains equipped with RBV exhibited only a marginal increase in activity as compared to the pristine PHPMA (cf. Fig. 10). In contrast, with PAA it was possible to achieve a pronounced inhibition of synthesis of the viral RNA in the absence of cytotoxic effects. In fact, the pristine polymer with no drug was able to afford an over 50% decrease in the expression of the viral genome — being better than the treatment based on free RBV. With RBV functionalization, the MP afforded a further significant increase in antiviral activity, this effect being statistically significant ($P < 0.01$) in the range of polymer concentration from 0.5 to 1 g/L. With the PAA–RBV conjugate, it was possible to achieve a near 80% inhibition of HCV RNA synthesis, with only a minor associated toxic effect. This effect cannot be achieved with RBV alone. For INF-α, the magnitude of this therapeutic effect is observed at a dose of 10 U/mL.

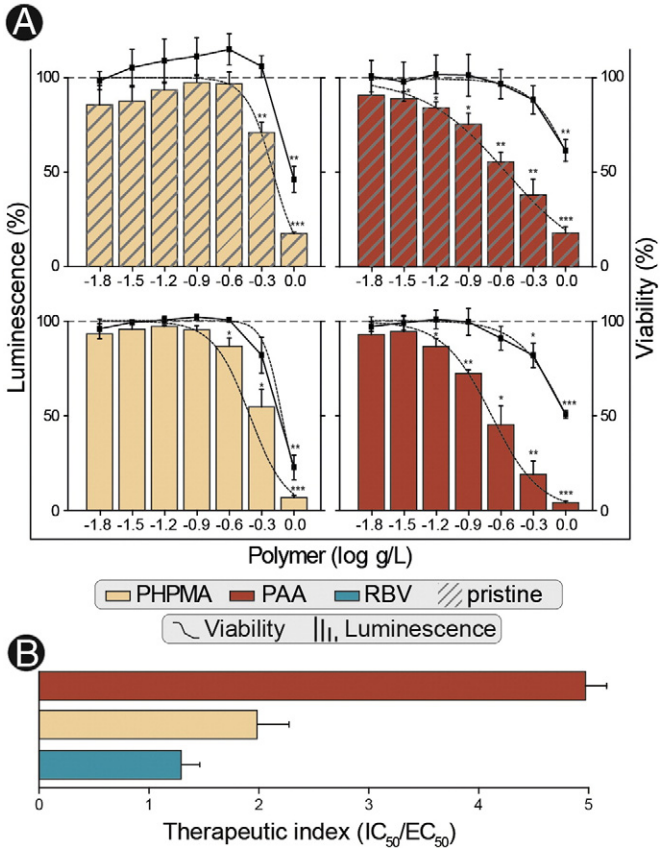

Fig. 10. A) Dose-dependent activity of macromolecular prodrugs of RBV in a HuH7-HCV replicon system following 48 h of incubation. A PAA–MP (8 kDa, 9 mol%) and a PHPMA–MP (7 kDa, 12 mol%) and their corresponding pristine control polymers were tested at a concentration range from 16 mg/L to 1 g/L. Shown results are the average of three independent experiments (n = 3). Statistical significance is given compared to the negative control. *P < 0.05, **P < 0.01, and ***P < 0.001. B) Therapeutic index for the two MPs in comparison to free RBV as calculated from the IC_{50}/EC_{50} ratio obtained from the dose–response curves through non-linear fitting (see dotted lines in A and Table SI6).

With regard to the activity of pristine PAA, we note that polyanions have a well-documented activity in preventing viral cell entry [13]. For both PAA and PMAA, this effect was first described *in vivo* in the late 1960s [35,36]. However, the replicon system as employed herein addresses solely the intracellular part of the viral life cycle and the activity of PAA is therefore different from the mechanisms described previously. In recent reports from our laboratory [39] and the De Clercq group [48,49] it was observed that linear and dendritic polymers have an intracellular activity against the proliferation of HIV, plausibly through inhibition of the viral polymerase (and/or integrase). Given the similarities between HCV and HIV with regard to the drug targets [2], it is plausible that the intracellular effect of PAA against HCV replication has a similar origin and mechanism of action. To our knowledge, this is the first report on the intracellular activity of polyanions directly affecting the proliferation of HCV. For PAA-based MPs of RBV, the inherent activity of the polymer contributes significantly to the overall activity of the formulation.

4. Conclusion and outlook

Macromolecular prodrugs have proven themselves as effective formulations to improve the pharmacology of the unique broad-spectrum antiviral agent, ribavirin. Across the macromolecular space (*i.e.* defined by polymer molar mass, drug loading, and carrier) MPs effectively elicited intracellular therapeutic responses in macrophages and, importantly, decreased drug-associated toxicity. The major factor in determining the potency of individual formulations was found to be the carrier polymer. Decreasing M_n and increasing drug loading resulted in higher potency of MPs, but this was generally accompanied with increased toxicity. Among the studied carriers, PAA based MPs were most potent and EC_{50} values approached those of the free drug. In regard to direct antiviral activity in a replicon system in hepatocytes, we provide the first evidence for direct, intracellular activity of the polymers against the replication of the viral RNA. For PAA, this contributed significantly to the potency of MPs. In a broad range of concentrations, a PAA–RBV conjugate significantly decreased the replication of the HCV replicon in the absence of noticeable toxicity.

Taken together, our recent work puts the negatively charged polymers and specifically PAA-based MPs back into the spotlight of research into macromolecular antiviral therapeutics. Negatively charged polymers have failed in the past in clinical trials due to side effects and limited *in vivo* efficacy [8,50]. However, these studies have preceded the advent of controlled radical polymerization techniques and earlier failures were arguably associated with poor quality of the macromolecules used (*i.e.* large polydispersity and batch-to-batch variation). Indeed, well-defined negatively charged carriers (*i.e.* poly(glutamic acid)) remain strong candidates in current clinical trials for delivery of

anticancer drugs [51,52]. Recent commercialization of negatively charged polymers (dendrimers) as microbicides for prevention of viral infectivity [53] also highlights the promise of macromolecules as antiviral agents. Further significant work is warranted to (dis)prove the safety of MPs for the delivery of antiviral drugs. However, we believe that our data on concurrent activity of PAA–RBV against both, HCV replication in hepatocytes and inflammation in macrophages makes these agents worthy of multiangle (pre)clinical investigation.

Acknowledgments

This work is supported by a grant from the Lundbeck Foundation and Sapere Aude Starting Grant from the Danish Council for Independent Research, Technology and Production Sciences, Denmark.

Appendix A. Supplementary data

Supplementary data to this article can be found online at http://dx.doi.org/10.1016/j.jconrel.2014.09.032.

References

[1] E. De Clercq, Antiviral agents active against influenza A viruses, Nat. Rev. Drug Discov. 5 (2006) 1015–1025.
[2] E. De Clercq, The design of drugs for HIV and HCV, Nat. Rev. Drug Discov. 6 (2007) 1001–1018.
[3] G.J. Dore, G.V. Matthews, J. Rockstroh, Future of hepatitis C therapy: development of direct-acting antivirals, Curr. Opin. HIV AIDS 6 (2011) 508–513.
[4] M.W. Fried, S.J. Hadziyannis, Treatment of chronic hepatitis C infection with peginterferons plus ribavirin, Semin. Liver Dis. 24 (2004) 47–54.
[5] B.E. Gilbert, V. Knight, Biochemistry and clinical applications of ribavirin, Antimicrob. Agents Chemother. 30 (1986) 201–205.
[6] R. Duncan, Polymer conjugates as anticancer nanomedicines, Nat. Rev. Cancer 6 (2006) 688–701.
[7] R. Duncan, The dawning era of polymer therapeutics, Nat. Rev. Drug Discov. 2 (2003) 347–360.
[8] F. Kratz, I.A. Müller, C. Ryppa, A. Warnecke, Prodrug strategies in anticancer chemotherapy, ChemMedChem 3 (2008) 20–53.
[9] J. Kopecek, P. Kopeckova, HPMA copolymers: origins, early developments, present, and future, Adv. Drug Deliv. Rev. 62 (2010) 122–149.
[10] G. Di Stefano, F.P. Colonna, A. Bongini, C. Busi, A. Mattioli, L. Fiume, Ribavirin conjugated with lactosaminated poly-L-lysine. Selective delivery to the liver and increased antiviral activity in mice with viral hepatitis, Biochem. Pharmacol. 54 (1997) 357–363.
[11] G. Levy, G. Adamson, M. Phillips, L. Scrocchi, L. Fung, P. Biessels, N. Ng, A. Ghanekar, A. Rowe, M. Ma, A. Levy, C. Koscik, W. He, R. Gorczynski, S. Brookes, C. Woods, I. McGilvray, D. Bell, Targeted delivery of ribavirin improves outcome of murine viral fulminant hepatitis via enhanced anti-viral activity, Hepatology 43 (2006) 581–591 (Baltimore, MD).
[12] A.A.A. Smith, B.M. Wohl, M.B.L. Kryger, N. Hedemann, C. Guerrero-Sanchez, A. Postma, A.N. Zelikin, Macromolecular prodrugs of ribavirin: concerted efforts of the carrier and the drug, Adv. Healthcare Mater. 3 (2014) 1404–1407.
[13] A. Smith, M. Kryger, B. Wohl, P. Ruiz-Sanchis, K. Zuwala, M. Tolstrup, A. Zelikin, Macromolecular (pro)drugs in antiviral research, Polym. Chem. (2014), http://dx.doi.org/10.1039/C4PY00624K.
[14] M.A. Gauthier, M.I. Gibson, H.A. Klok, Synthesis of functional polymers by post-polymerization modification, Angew. Chem. Int. Ed. 48 (2009) 48–58.
[15] B.K. Liu, N. Wang, Q. Wu, C.Y. Xie, X.F. Lin, Regioselective enzymatic acylation of ribavirin to give potential multifunctional derivatives, Biotechnol. Lett. 27 (2005) 717–720.
[16] X. Li, Q. Wu, M. Lu, F. Zhang, X.F. Lin, Novel hepatoma-targeting micelles based on chemo-enzymatic synthesis and self-assembly of galactose-functionalized ribavirin-containing amphiphilic random copolymer, J. Polym. Sci. A Polym. Chem. 46 (2008) 2734–2744.
[17] M.B.L. Kryger, A.A.A. Smith, B.M. Wohl, A.N. Zelikin, Macromolecular prodrugs for controlled delivery of ribavirin, Macromol. Biosci. 14 (2013) 173–185.
[18] M.B.L. Kryger, B.M. Wohl, A.A.A. Smith, A.N. Zelikin, Macromolecular prodrugs of ribavirin combat side effects and toxicity with no loss of activity of the drug, Chem. Commun. 49 (2013) 2643–2645.
[19] B.M. Wohl, A.A.A. Smith, M.B.L. Kryger, A.N. Zelikin, Narrow therapeutic window of ribavirin as an inhibitor of nitric oxide synthesis is broadened by macromolecular prodrugs, Biomacromolecules 14 (2013) 3916–3926.
[20] V. Lohmann, F. Körner, J.O. Koch, U. Herian, L. Theilmann, R. Bartenschlager, Replication of subgenomic hepatitis C virus RNAs in a hepatoma cell line, Science 285 (1999) 110–113.
[21] K.J. Blight, J.A. McKeating, C.M. Rice, Highly permissive cell lines for subgenomic and genomic hepatitis C virus RNA replication, J. Virol. 76 (2002) 13001–13014.
[22] P. Ruiz-Sanchis, B.M. Wohl, A.A.A. Smith, K. Zuwala, J. Melchjorsen, M. Tolstrup, A.N. Zelikin, Highly active macromolecular prodrugs inhibit expression of the hepatitis C virus genome in the host cells, Adv. Healthcare Mater. (2014), http://dx.doi.org/10.1002/adhm.201400307.
[23] A. Tsubota, N. Akuta, F. Suzuki, Y. Suzuki, T. Someya, M. Kobayashi, Y. Arase, S. Saitoh, K. Ikeda, H. Kumada, Viral dynamics and pharmacokinetics in combined interferon alfa-2b and ribavirin therapy for patients infected with hepatitis C virus of genotype 1b and high pretreatment viral load, Intervirology 45 (2002) 33–42.
[24] J.J. Feld, J.H. Hoofnagle, Mechanism of action of interferon and ribavirin in treatment of hepatitis C, Nature 436 (2005) 967–972.
[25] E. De Clercq, Ribavirin for HIV, Lancet 338 (1991) 450–451.
[26] R.E. Kast, Ribavirin in cancer immunotherapies: controlling nitric oxide augments cytotoxic lymphocyte function, Neoplasia 5 (2003) 3–8.
[27] T. Akaike, H. Maeda, Nitric oxide and virus infection, Immunology 101 (2000) 300–308.
[28] S. Perrier, P. Takolpuckdee, C.A. Mars, Reversible addition–fragmentation chain transfer polymerization: end group modification for functionalized polymers and chain transfer agent recovery, Macromolecules 38 (2005) 2033–2036.
[29] M.J. Moorcroft, J. Davis, R.G. Compton, Detection and determination of nitrate and nitrite: a review, Talanta 54 (2001) 785–803.
[30] U. Forstermann, H. Kleinert, Nitric oxide synthase: expression and expressional control of the three isoforms, Naunyn-Schmiedeberg's Arch. Pharmacol. 352 (1995) 351–364.
[31] M. Michaelis, R. Michaelis, T. Suhan, H. Schmidt, A. Mohamed, H.W. Doerr, J. Cinatl Jr., Ribavirin inhibits angiogenesis by tetrahydrobiopterin depletion, FASEB J. 21 (2007) 81–87.
[32] F. Gobeil, T. Zhu, S. Brault, A. Geha, A. Vazquez-Tello, A. Fortier, D. Barbaz, D. Checchin, X. Hou, M. Nader, G. Bkaily, J.P. Gratton, N. Heveker, A. Ribeiro-da-Silva, K. Peri, H. Bard, A. Chorvatova, P. D'Orleans-Juste, E.J. Goetzl, S. Chemtob, Nitric oxide signaling via nuclearized endothelial nitric-oxide synthase modulates expression of the immediate early genes iNOS and mPGES-1, J. Biol. Chem. 281 (2006) 16058–16067.
[33] D. Pissuwan, C. Boyer, K. Gunasekaran, T.P. Davis, V. Bulmus, *In vitro* cytotoxicity of RAFT polymers, Biomacromolecules 11 (2010) 412–420.
[34] C.W. Chang, E. Bays, L. Tao, S.N.S. Alconcel, H.D. Maynard, Differences in cytotoxicity of poly(PEGA)s synthesized by reversible addition–fragmentation chain transfer polymerization, Chem. Commun. (2009) 3580–3582.
[35] P. De Somer, E. De Clercq, A. Billiau, E. Schonne, M. Claesen, Antiviral activity of polyacrylic and polymethacrylic acids. I. Mode of action *in vitro*, J. Virol. 2 (1968) 878–885.
[36] P. De Somer, E. De Clercq, A. Billiau, E. Schonne, M. Claesen, Antiviral activity of polyacrylic and polymethacrylic acids. II. Mode of action *in vivo*, J. Virol. 2 (1968) 886–893.
[37] L.A.T. Hilgers, I. Nicolas, G. Lejeune, E. Dewil, B. Boon, Effect of various adjuvants on secondary immune response in chickens, Vet. Immunol. Immunopathol. 66 (1998) 159–171.
[38] Y.K. Chong, G. Moad, E. Rizzardo, S.H. Thang, Thiocarbonylthio end group removal from RAFT-synthesized polymers by radical-induced reduction, Macromolecules 40 (2007) 4446–4455.
[39] K. Zuwala, A.A.A. Smith, A. Postma, C. Guerrero-Sanchez, P. Ruiz-Sanchis, J. Melchjorsen, M. Tolstrup, A.N. Zelikin, Polymers fight HIV: potent (pro)drugs identified through parallel automated synthesis, Adv. Healthcare Mater. (2014), http://dx.doi.org/10.1002/adhm.
[40] R. Zeng, Z. Wang, H. Wang, L. Chen, L. Yang, R. Qiao, L. Hu, Z. Li, Effect of bond linkage on *in vitro* drug release and anti-HIV activity of chitosan–stavudine conjugates, Macromol. Res. 20 (2012) 358–365.
[41] W. Li, Y. Chang, P. Zhan, N. Zhang, X. Liu, C. Pannecouque, E. De Clercq, Synthesis, *in vitro* and *in vivo* release kinetics, and anti-HIV activity of a sustained-release prodrug (mPEG-AZT) of 3′-azido-3′-deoxythymidine (AZT, Zidovudine), ChemMedChem 5 (2010) 1893–1898.
[42] L. Yang, L. Chen, R. Zeng, C. Li, R. Qiao, L. Hu, Z. Li, Synthesis, nanosizing and *in vitro* drug release of a novel anti-HIV polymeric prodrug: chitosan–O-isopropyl-5′-O-d4T monophosphate conjugate, Bioorg. Med. Chem. 18 (2010) 117–123.
[43] P. Vlieghe, T. Clerc, C. Pannecouque, M. Witvrouw, E. De Clercq, J.-P. Salles, J.-L. Kraus, Synthesis of new covalently bound kappa-carrageenan–AZT conjugates with improved anti-HIV activities, J. Med. Chem. 45 (2002) 1275–1283.
[44] M.-A. Yessine, J.-C. Leroux, Membrane-destabilizing polyanions: interaction with lipid bilayers and endosomal escape of biomacromolecules, Adv. Drug Deliv. Rev. 56 (2004) 999–1021.
[45] T. Etrych, L. Kovář, J. Strohalm, P. Chytil, B. Říhová, K. Ulbrich, Biodegradable star HPMA polymer–drug conjugates: biodegradability, distribution and anti-tumor efficacy, J. Control. Release 154 (2011) 241–248.
[46] M.K. Jain, C. Zoellner, Role of ribavirin in HCV treatment response: now and in the future, Expert. Opin. Pharmacother. 11 (2010) 673–683.
[47] T. Kato, T. Date, M. Miyamoto, M. Sugiyama, Y. Tanaka, E. Orito, T. Ohno, K. Sugihara, I. Hasegawa, K. Fujiwara, K. Ito, A. Ozasa, M. Mizokami, T. Wakita, Detection of anti-hepatitis C virus effects of interferon and ribavirin by a sensitive replicon system, J. Clin. Microbiol. 43 (2005) 5679–5684.
[48] M. Witvrouw, V. Fikkert, W. Pluymers, B. Matthews, K. Mardel, D. Schols, J. Raff, Z. Debyser, E. De Clercq, G. Holan, C. Pannecouque, Polyanionic (i.e., polysulfonate) dendrimers can inhibit the replication of human immunodeficiency virus by interfering with both virus adsorption and later steps (reverse transcriptase/integrase) in the virus replicative cycle, Mol. Pharmacol. 58 (2000) 1100–1108.
[49] Y. Gong, B. Matthews, D. Cheung, T. Tam, I. Gadawski, D. Leung, G. Holan, J. Raff, S. Sacks, Evidence of dual sites of action of dendrimers: SPL-2999 inhibits both virus entry and late stages of herpes simplex virus replication, Antivir. Res. 55 (2002) 319–329.
[50] V. Pirrone, B. Wigdahl, F.C. Krebs, The rise and fall of polyanionic inhibitors of the human immunodeficiency virus type 1, Antivir. Res. 90 (2011) 168–182.
[51] C. Li, S. Wallace, Polymer–drug conjugates: recent development in clinical oncology, Adv. Drug Deliv. Rev. 60 (2008) 886–898.

[52] X. Pang, H.-L. Du, H.-Q. Zhang, Y.-J. Zhai, G.-X. Zhai, Polymer–drug conjugates: present state of play and future perspectives, Drug Discov. Today 18 (2013) 1316–1322.
[53] R. Duncan, Polymer therapeutics: top 10 selling pharmaceuticals — what next? J. Control. Release 190 (2014) 371–380.
[54] A.A.A. Smith, K. Zuwala, M.B.L. Kryger, B.M. Wohl, C. Guerrero-Sanchez, M. Tolstrup, A. Postma, A.N. Zelikin, Macromolecular prodrugs of ribavirin: Towards a treatment for co-infection with HIV and HCV, Chem. Sci. (2014), http://dx.doi.org/10.1039/C4SC02754J.